

ARTICLE OPEN



High strength bio-concrete for the production of building components

Maiia Smirnova¹, Christoph Nething^{1✉}, Andreas Stolz², Janosch A. D. Gröning², Daniele P. Funaro², Erik Eppinger², Manuela Reichert³, Jürgen Frick³ and Lucio Blandini¹

The production of bio-concrete is based on the process of microbially-induced calcium carbonate precipitation (MICP), in which calcium carbonate (CaCO₃) is formed as a binder. Bio-concrete is a potentially CO₂-neutral alternative to conventional Portland-cement-based concrete, since no process-related carbon dioxide emissions are generated during biomineralization. Furthermore, CO₂ is bound in the form of carbonate. However, achieving compressive strength values comparable to conventional concrete, in combination with sufficient component depth, has been a significant challenge in the MICP research. In the present study, a combination of methods was implemented, including the use of urease-active calcium carbonate powder (UACP) instead of free bacterial cells, optimization of aggregate packing density, and the implementation of an automated stop-flow pressure injection method. A variety of cementation parameters were tested to determine the optimal conditions for the production of homogeneously cemented high strength bio-concrete. Additionally, reproducibility and optimization studies have been conducted with selected parameter combinations. It was found that achieving homogeneous compaction with sufficient aggregate packing density played a crucial role in obtaining consistent and high-quality cementation results. A combination of a very high compressive strength of 52.5 MPa and a cementation depth of 140 mm has been reached, which has not been reported in previous publications. These findings might unveil new possibilities for bio-concrete to be used in the production of prefabricated load-bearing building components, where it could partially replace traditional concrete.

npj Materials Sustainability (2023)1:4; <https://doi.org/10.1038/s44296-023-00004-6>

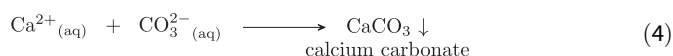
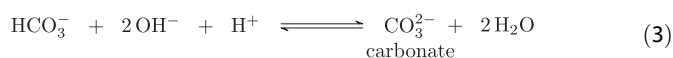
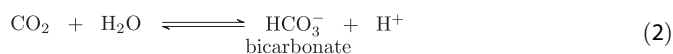
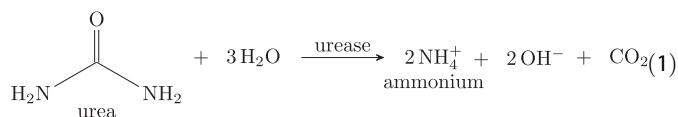
INTRODUCTION

Portland-cement-based concrete is a crucial building material in modern construction. According to the International Energy Agency (IEA) the carbon dioxide emissions from cement production have not changed after an increase in 2018 and remained high in 2022 (ca. 0.6 t CO₂ per tonne of cement¹). Consequently, the production of cement, contributes to around 7 to 8% of the global CO₂ emissions^{2,3}. Even though energy-related emissions can be reduced by shifting to renewable energy sources, process emissions from the calcination of limestone cannot be eliminated entirely. Clinker substitution is often used to tackle the problem of process emissions, but this still falls within the traditional clinker-based cement paradigm.

Bio-concrete represents a different approach, in which aggregates are consolidated by calcium carbonate crystals produced through microbially-induced calcium carbonate precipitation (MICP). The biomineralization through MICP is CO₂-negative, as carbon dioxide is stored in carbonate compounds. Bio-concrete has a chemical composition similar to calcite-cemented sandstone and can be shaped into various forms and reinforced, making it potentially suitable for the production of larger building components. By producing raw materials with renewable energy sources and circular economy principles, bio-concrete could, therefore, be considered a CO₂-neutral alternative to the Portland-cement-based concrete.

Ureolytic bacteria are used in bio-concrete to initiate the formation of calcium carbonate crystals after the addition of urea and calcium salts⁴. The enzyme urease hydrolyzes urea and acts as a catalyst for the calcium carbonate precipitation (Eq. (1)). In the

urease reaction (in dependence of the pH) carbonate and hydrogen carbonate ions are formed. Furthermore, the inter-conversion of CO₂ and hydrogen carbonate (plus H⁺) can also be catalyzed by the enzyme carbonic anhydrase (Eq. (2)⁵). One consequence of the urea degradation is the formation of ammonia which reacts in aqueous solutions to ammonium and hydroxide ions (Eq. (1))⁶. The pH value increases due to the increasing concentration of hydroxide ions, which leads to an increased concentration of carbonate ions in the solution (Eq. (3)). If a calcium salt is present, calcium carbonate precipitates (Eq. (4)):



Unlike purely chemical processes that lead to the rapid spontaneous precipitation of calcium carbonate, MICP is characterized by local successive increases and decreases of pH levels⁷. This results in the growth of stable calcium carbonate crystals over time, where bacterial cells act as crystallization nuclei⁸.

MICP is already being applied in some areas of construction, such as self-healing (Portland-cement-based) concrete⁹, soil

¹Institute for Lightweight Structures and Conceptual Design, University of Stuttgart, Stuttgart, Germany. ²Institute of Microbiology, University of Stuttgart, Stuttgart, Germany. ³Materials Testing Institute, University of Stuttgart, Stuttgart, Germany. ✉email: christoph.nething@ilek.uni-stuttgart.de

consolidation¹⁰, and the production of bio-bricks^{11,12}. This technology could be implemented in various ways to meet different sustainable development goals of the United Nations¹³. However, the application of MICP for the production of building components remains challenging, since compressive strength values comparable to those of concrete in conjunction with sufficient component depth has not yet been achieved. Overcoming these obstacles is the main goal of the presented research.

There is a positive correlation between the compressive strength of biomineralized specimens and the amount of precipitated calcium carbonate¹⁴. MICP takes place in an aqueous environment and the amount of precipitated material is limited by the solubility of the reactants and microbiological factors. Hence, the aggregate pore volume can only be partially filled with calcium carbonate after a single supply of the cementation solution containing urea and calcium ions. Therefore, the cementation solution in the pore space between aggregates needs to be continuously or repeatedly replaced during biomineralization. The flow of the cementation solution through the aggregate matrix can lead to inhomogeneous cementation over time due to various factors, including bacterial transport^{15,16}, chemical depletion along the flow path and clogging near the entry point of the cementation solution¹⁷.

Cheng and Shahin proposed a method to restrict bacterial transport in the sand matrix through the production of “bioslurry”¹⁸. In this method, bacteria are embedded in calcium carbonate crystals via MICP. The resulting “slurry” is then mixed with aggregates and is reported to improve the retention of bacteria during cementation. Due to the embedding of the bacterial cells in calcium carbonate, ~95% of the urease activity present in the UACP preparation is retained during percolation of the sample bodies¹⁸. In contrast, it was found that up to 75% of bacterial cells were flushed out during biomineralization when pure bacterial suspensions were used¹⁶. Nething et al. further processed the “bioslurry” into an urease-active calcium carbonate powder (UACP) by freeze-drying, which allowed the long-term storage of the urease-active material¹⁹.

Although significant advances in MICP have been described throughout the last years, it is still challenging to achieve compressive strength values comparable to conventional concrete, along with sufficient component depth. By maximizing the aggregate packing density and revealing the dependencies between different cementation parameters this study proves the possibility of producing high strength bio-concrete with unconfined compressive strength values higher than 50 MPa and sufficient cementation depth of 140 mm.

RESULTS

Aggregate packing density

One-dimensional compression strength tests have shown that in MICP-treated sand, at the micro level, the bonds between the calcium carbonate and the aggregates break first, followed by the destruction of calcium carbonate crystals and ultimately the breakage of aggregates²⁰. Maximizing the aggregate content is therefore crucial for achieving high compressive strength of the biocemented material. Packing density optimization allows to increase the volume ratio of aggregates to voids in the mix, which also brings economical benefits due to the reduced consumption of the cementation solution.

The packing density optimization was carried out with six different quartz sand fractions ([0.063–0.25 mm], [0.1–0.4 mm], [0.2–0.6 mm], [0.3–0.8 mm], [0.7–1.25 mm] and [1.0–2.0 mm] with the grain density 2.65 g/cm³, each), obtained from Holcim Kies und Beton GmbH. The Elkem Material Mix Analyser (EMMA) software was used to generate a grading curve with an optimized packing density based on the Modified Andreasen model. The

grading curve was designed only with respect to the aggregate content disregarding the finer UACP particles. It was assumed that the low amount of UACP with particle sizes of 3 to 15 μm would not affect the aggregate packing density. The resulting grading curve is shown in Fig. 1A.

Subsequently, compaction experiments were carried out to compare the packing density of the optimized mix with homogeneous aggregates, along with UACP. The volume compositions of the mixes after compaction were determined based on their weights, the mass fractions of the mix components and the densities of the respective materials.

Two parameters were employed to characterize the packing density in the compacted specimen. The first parameter, denoted as $\varphi_{\text{aggr}+\text{UACP}}$, quantified the porosity. It represented the initial pore volume, free from both aggregates and UACP, which was filled with the cementation solution and air prior to the biomineralization process. The second parameter, φ_{aggr} , described the space between the aggregates as if no UACP was present in the specimen. The lower the value of φ_{aggr} the higher the aggregate packing density, which represented the preferable condition.

The compacted specimens with 1.5% (w/w relative to the dry mix (without cementation solution), further denoted as w/w_{dm}) UACP with the applied compaction pressure of 5 N/mm² showed values of φ_{aggr} from 0.45 to 0.47, when the separate homogeneous sand fractions listed in Fig. 1A were used as aggregates. However, the lowest value of $\varphi_{\text{aggr}} = 0.35$ of all the compacted specimens was achieved, when the optimized mix was used instead. Therefore, the optimized mix with 1.5% (w/w_{dm}) UACP exhibited higher aggregate packing density, than the mixes with separate homogeneous sand fractions and the same amounts of UACP. Examples of volume compositions with 0.1–0.4 mm sand and the optimized mix are shown in Fig. 1B.

Although it was possible to further reduce the pore volume by incorporating lime fines into the mix design, it would however hinder the flow of the cementation solution through the mixes in the stop-flow injection method. Therefore, the fines were excluded from the mix design in the current study (see “Discussion”).

Biomineralization experiments

In the following, the optimized aggregate mixes were used for biomineralization experiments.

Initially, percolation by gravity was applied as previously described by Nething et al.¹⁹. The percolation with 18 4-h-cycles of the mixes with 1.5% (w/w_{dm}) UACP resulted in a limited cementation depth of less than 40 mm. In addition, the experiments showed only a low degree of reproducibility.

Cheng and Cord-Ruwisch suggested that deeper and more homogeneous cementation could be achieved by increasing the flow rate of the cementation solution¹⁷. A stop-flow pressure-based injection method was therefore applied to produce biomineralized specimens with higher cementation depths.

For biomineralization, the mixes with aggregates and UACP were prepared and compacted into cylindrical formworks ($D = 50\text{--}53.3$ mm, $H = 150$ mm, specimen height $H_s = 135\text{--}140$ mm) as described in “Methods”.

An automated pressure-based cementation system (Fig. 2) was implemented to feed cementation solutions from the bottom into the formworks at regular time intervals of 4 h using different pressures. The number of cycles varied between different test series, ranging from 18 to 28. This setup enabled the simultaneous production of six bio-cemented specimens. A detailed description of the setup is provided in “Methods”.

The following biomineralization experiments were conducted with this system:

- Test series 1–5: these tests aimed to evaluate the impact of various cementation conditions, such as pressure and

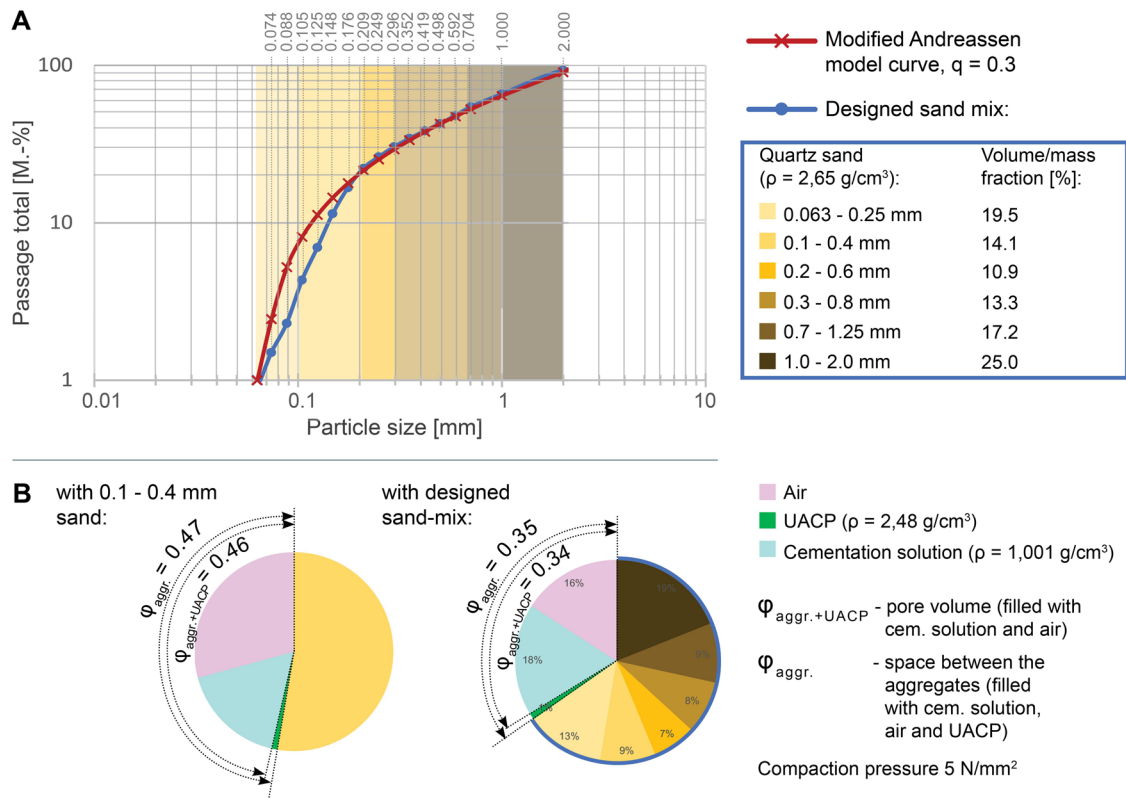


Fig. 1 Aggregate packing density optimization. **A** Grading curve of the optimized sand mix with grain sizes of 0.063–2 mm (blue) in comparison to the theoretical Andreassen-curve (red). **B** Volume compositions of mixes with 1.5% (w/w_{dm}) UACP in the compacted specimen.

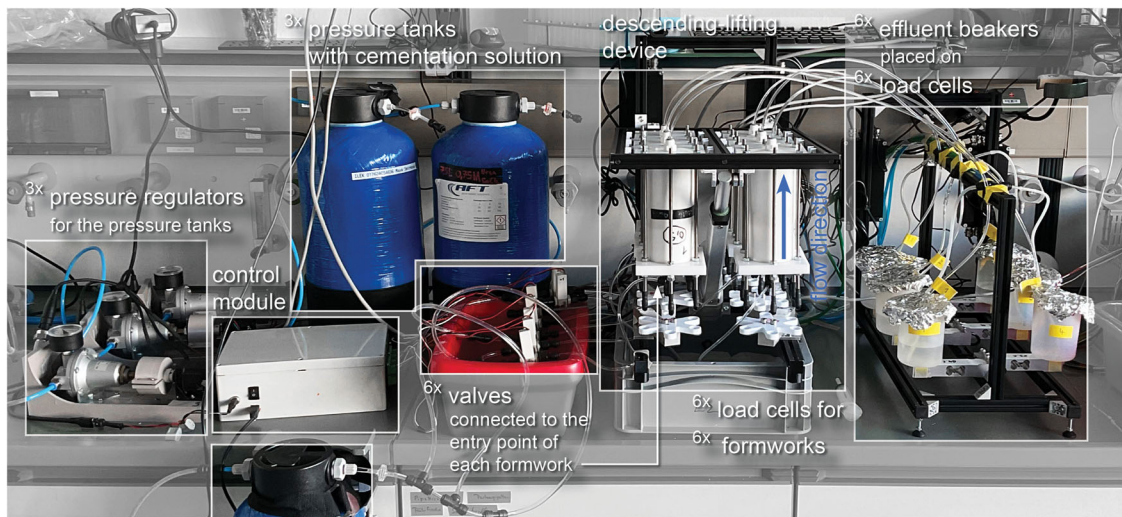


Fig. 2 Automated pressure-based cementation system. The system allows simultaneous biomineralization of six specimens.

concentration of the cementation solution, on the depth and compressive strength of the biomineralized specimens. The specimens were produced using the optimized aggregate mix with different amounts of UACP.

- Test series 6 and 7: these tests were carried out to assess the reproducibility of the biomineralization method using one of the optimal parameter combinations identified in test series 1 to 5. In order to further optimize cementation conditions and achieve maximal homogeneity and strength of the produced specimens, a higher compaction pressure was applied and a step-wise increase of the supply pressure was tested in test series 7.

Cementation conditions and urease activity of all produced specimens are shown in Table 1. Extended data, including specimen masses, as well as compaction pressures, estimated values of $\phi_{\text{aggr}+\text{UACP}}$, ϕ_{aggr} and initial pore volumes are provided in Supplementary Table 1.

Biomineralization under various cementation conditions (test series 1–5)

The specimens of test series 1–5 were produced with 0.5%–7.5% (w/w_{dm}) UACP. The supply pressure of the cementation solution was varied between 0.1 and 0.75 bar. The concentration of the

Table 1. Mix compositions and treatment systems used during the stop-flow biomineralization experiments.

Test series N	Urease activity [U/mg UACP] ^a	Specimen name	UACP [% (w/wdm)]	Cc.s. [M]	P [bar]
1 (var. UACP %)	0.31 ± 0.04	1.1	0.5	0.75	0.1
"	"	1.2	1.0	"	"
"	"	1.3	2.0	"	"
"	"	1.4	2.5	"	"
"	"	1.5	5.0	"	"
"	"	1.6	7.5	"	"
2 (var. UACP %, p)	0.25 ± 0.01	2.1	2.0	0.75	0.2
"	"	2.2	2.5	"	"
"	"	2.3	5.0	"	"
"	"	2.4	2.0	"	0.3
"	"	2.5	2.5	"	"
"	"	2.6	5.0	"	"
3 (var. C _{c.s.} , p)	0.30 ± 0.02	3.1, 3.2	2.0	0.75	0.1
"	"	3.3, 3.4	"	1.25	"
"	"	3.5, 3.6	"	0.75	0.5
4 (var. C _{c.s.} , p)	0.30 ± 0.02	4.1, 4.2	1.5	0.75	0.1
"	"	4.3, 4.4	"	1.5	"
"	"	4.5, 4.6	"	0.75	0.25
5 (var. p)	0.60 ± 0.01	5.1, 5.2	1.5	0.75	0.25
"	"	5.3, 5.4	"	"	0.5
"	"	5.5, 5.6	"	"	0.75
6 (reprod. of spec. 1.2)	0.56 ± 0.08	6.1/.2/.3/.4/.5/.6	1.0	0.75	0.1
7 (lower ϕ_{aggr} step-wise p)	0.71 ± 0.09	7.1/.2/.3/.4/.5/.6	1.0	0.75	0.1–1

C_{c.s.} concentration of the used cementation solution (equimolar urea and calcium chloride), p supply pressure of the cementation solution.
^aSee Methods, "Urease activity of the UACP".

cementation solution was 0.75 M (equimolar urea and calcium chloride) for most of the biomineralization experiments, except for the specimens 3.3/3.4 with 1.25 M and 4.3/4.4 with 1.5 M.

An example of the data collected during biomineralization of the specimens with 0.5, 1.0 and 1.5% (w/w_{dm}) UACP is presented in Fig. 3. The data for the rest of the specimens from test series 1–5 is provided in Supplementary Figs. 1–6.

The diagrams describing the weight changes of the specimens showed that curves for the experiments with the same amounts of UACP and the same applied external pressures exhibited similar slopes, indicating a similar rate of calcium carbonate production (Fig. 3). Most curves indicated a rapid increase in weight at the beginning of the cementation process, which could be attributed to the filling of pore volume, formwork cavities, and supply hoses by the cementation solution. Higher rates of calcium carbonate formation after the filling of pore volume are desirable due to the overall faster and more efficient production of biomineralized material.

The flow rate in all biomineralization experiments eventually approached a zero value, indicating clogging of the specimens. At that point, the rate of calcium carbonate production significantly decreased, as displayed by the kink in some weight increase diagrams (marked by the red arrows in Fig. 3B).

In certain experiments clogging occurred right from the beginning of the cementation process, which was indicated by

near zero flow rates and very slow rates of calcium carbonate formation (see Supplementary Figs. 1 and 2, specimens 2.2, 2.3, 2.6, 3.1 and 3.2). Similar behavior was observed in specimens 4.1, 4.2, 4.5, 4.6, 5.1 and 5.2 (Fig. 3B). As a result, all of those specimens were only partially biomineralized, as can be seen in Fig. 4.

Almost no urea or calcium ions were found in the effluent solutions from the beginning of the biomineralization experiments for the specimens containing 2, 2.5 and 5% (w/w_{dm}) UACP. This indicated that these chemicals were fully utilized in the biomineralization process. This observation is consistent with the ammonium concentration, which reached the maximum limit of 1.5 M for the cementation solution containing 0.75 M urea (Supplementary Fig. 4).

Higher concentrations of urea and calcium ions at the beginning of the biomineralization experiment were observed in the effluent solutions for the specimens containing 0.5, 1.0 and 1.5% (w/w_{dm}) UACP (Fig. 3). The decrease in these concentrations was observed until ~40–48 h followed by their increase in the biomineralization experiments 1.1, 1.2 and 5.3, which could be attributed to a decline in the urease activity. However, the concentration remained near zero for the specimens 5.4, 5.5 and 5.6, indicating the complete utilization of urea and calcium in the biomineralization process. The ammonium concentration reached its maximum value of 1.5 M for all specimens at different time points.

The images of the specimens obtained from test series 1–5 are presented in Fig. 4A and the corresponding cementation depth diagram in Fig. 4B. It was observed that specimens with the same UACP content exhibited an increase in cementation depth when the supply pressure of the cementation solution was increased. Fully biomineralized specimens ($H = 135$ mm) were produced using the following parameters (all produced with concentrations of urea and calcium chloride of 0.75 M, each):

- 0.5% (w/w_{dm}) UACP, 0.1 bar (specimen 1.1);
- 1.0% (w/w_{dm}) UACP, 0.1 bar (specimen 1.2);
- 1.5% (w/w_{dm}) UACP, 0.5/0.75 bar (specimens 5.3, 5.4, 5.5, 5.6);
- 7.5% (w/w_{dm}) UACP, 0.1 bar (specimen 1.6).

The unconfined compressive strength (UCS) values of the specimens produced in test series 1–5 are marked in Fig. 4A. Certain specimens exhibited very high UCS values, with a maximum of 57.4 MPa observed in the bottom part of specimen 5.6. This represented a significant strength improvement compared to other studies on bio-concrete (2 MPa by Bernardi et al.²¹, 1.3 MPa by Bu et al.¹², 9.7 MPa by Cheng et al.¹¹). However, it should be noted that inhomogeneities in UCS values were observed between the lower and upper parts of most specimens. Only two specimens, 1.2 and 5.3, displayed similar compressive strength values in both their lower and upper parts.

It was observed that the cementation depth decreased with the increasing UACP content up to 2% (w/w_{dm}). The very high UACP content of 7.5% (w/w_{dm}) had a negative impact on the biomineralization process, which was evident from the increase in the cementation depth and the decrease in the compressive strength of the specimen 1.6 compared to the specimens with the lower amount of UACP produced with similar parameters.

Ultrasonic wave velocity measurements were conducted on the selected deeply cemented specimens to further assess the homogeneity of the biomineralization. Measurements were conducted on the specimens that had already been cut to size for the UCS tests, and the corresponding values are marked in Fig. 4A. The observed ultrasonic wave velocity data correlated well with the UCS results obtained for these specimens.

The specimen 1.2 exhibited a highly homogeneous cementation, with ultrasonic wave velocities ranging from 4.50 to 4.64 km/s in the direction parallel to the compaction layers. While specimen 5.3 demonstrated slightly less homogeneity, it still displayed high ultrasonic wave velocities in the same direction, ranging from 4.31 to 4.64 km/s.

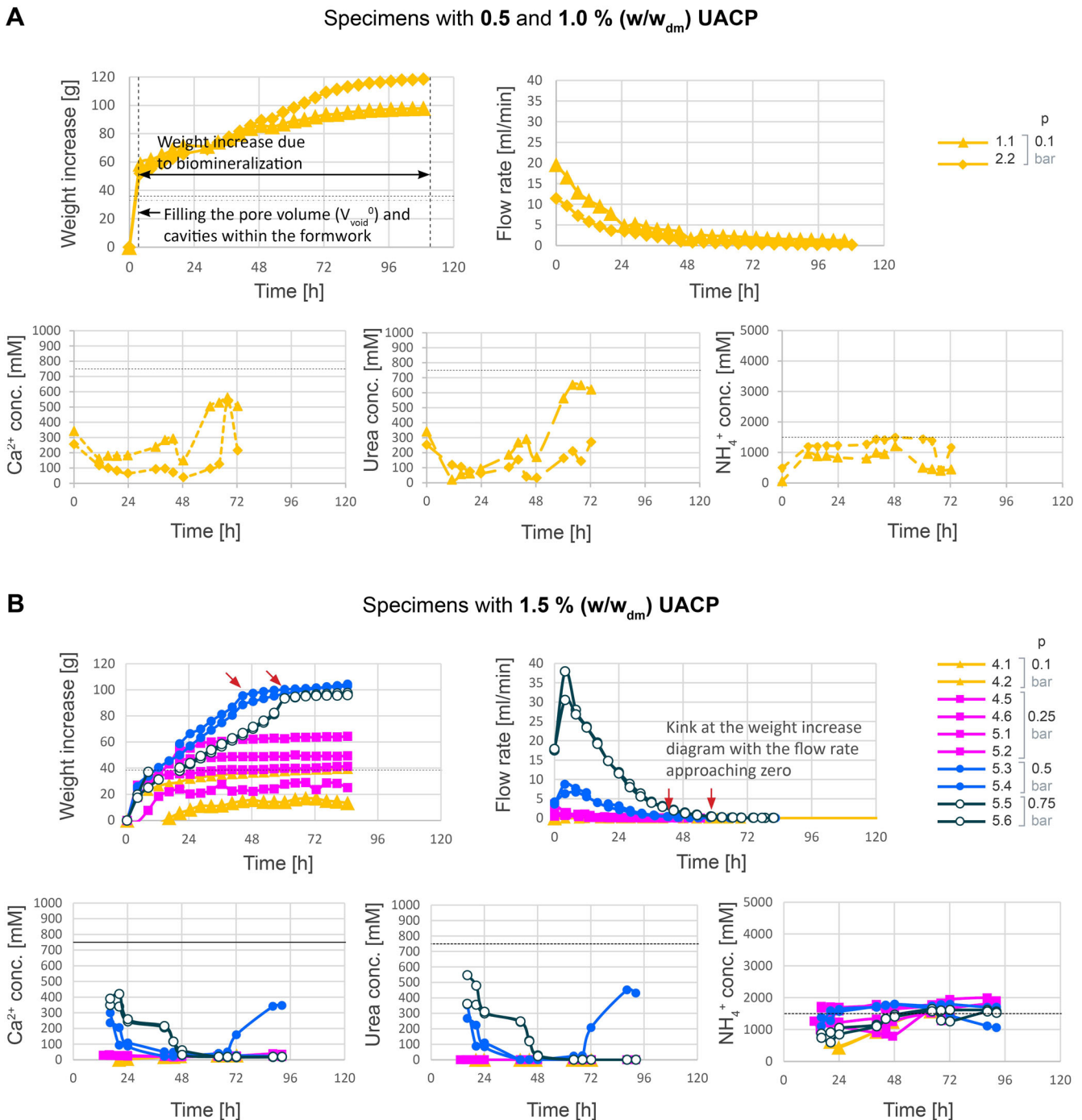


Fig. 3 Changes in specimen weights, flow rates, urea-, ammonium- and calcium-concentrations in the effluent solutions during biomineralization in test series 1-5. **A** Data for the experiments with 0.5 and 1.0% (w/w_{dm}) UACP. **B** Data for the experiments with 1.5% (w/w_{dm}) UACP.

Increasing the pressure from 0.5 bar (specimens 5.3 and 5.4) to 0.75 bar (specimens 5.5 and 5.6) did not improve the cementation speed, as indicated by the weight change diagrams (Fig. 3B). In the case of specimens 5.5 and 5.6, high flow rates of up to 40 ml/min may have negatively affected the distribution of calcium carbonate in the pore space, as observed in the ultrasonic wave velocity measurements (Supplementary Fig. 7).

The ultrasonic wave velocities measured in the direction perpendicular to the compaction layers were lower than the lowest value observed in the parallel direction for all the investigated specimens. This is comparable to the sedimentation

direction of natural sandstones, which as well exhibit anisotropy of ultrasonic wave velocity²² and implies a potential need for improvements in the compaction technique to achieve more uniform cementation in all directions.

Higher concentrations of the cementation solution resulted in a slightly increased cementation depth for the specimens produced with 1.5% (w/w_{dm}) UACP and 2% (w/w_{dm}) UACP (Fig. 4, specimens 3.1–3.2 vs. 3.3–3.4 and 4.1–4.2 vs. 4.3–4.4). Additionally, higher ammonium production was observed in the specimens with higher concentrations of the cementation solution (Supplementary Fig. 6).



Fig. 4 Biomineralized specimens produced in test series 1–5. A The UCS-measurements of the cut samples and the positions of the cuts are marked in the images of the specimens. The ultrasonic wave velocity measurements (*uwv, [km/s]) at the marked points are shown in the enlarged images of the specimens 1.2, 5.3 and 5.6. **B** The cementation depth diagram of all produced specimens sorted according to the amounts of UACP and applied pressures.

Reproducibility of the applied method (test series 6 and 7)

In the following test series 6, the parameter combination, which resulted in high UCS values and homogeneous cementation in test series 1 to 5 (specimen 1.2), was selected to test the reproducibility of the applied method ([0.5% (w/w_{dm}) UACP, 0.1

bar, 0.75 M urea and CaCl₂]). The compaction of the specimens resulted in a slightly lower aggregate packing density compared to the specimen 1.2 (aggregate packing density $\rho_{\text{aggr.}} = \text{ca. } 1.65\text{--}1.68$ vs. 1.74 g/cm^3 , which corresponds to $\phi_{\text{aggr.}} = \text{ca. } 0.37\text{--}0.38$ vs. 0.34). The ultrasonic wave velocity measurements

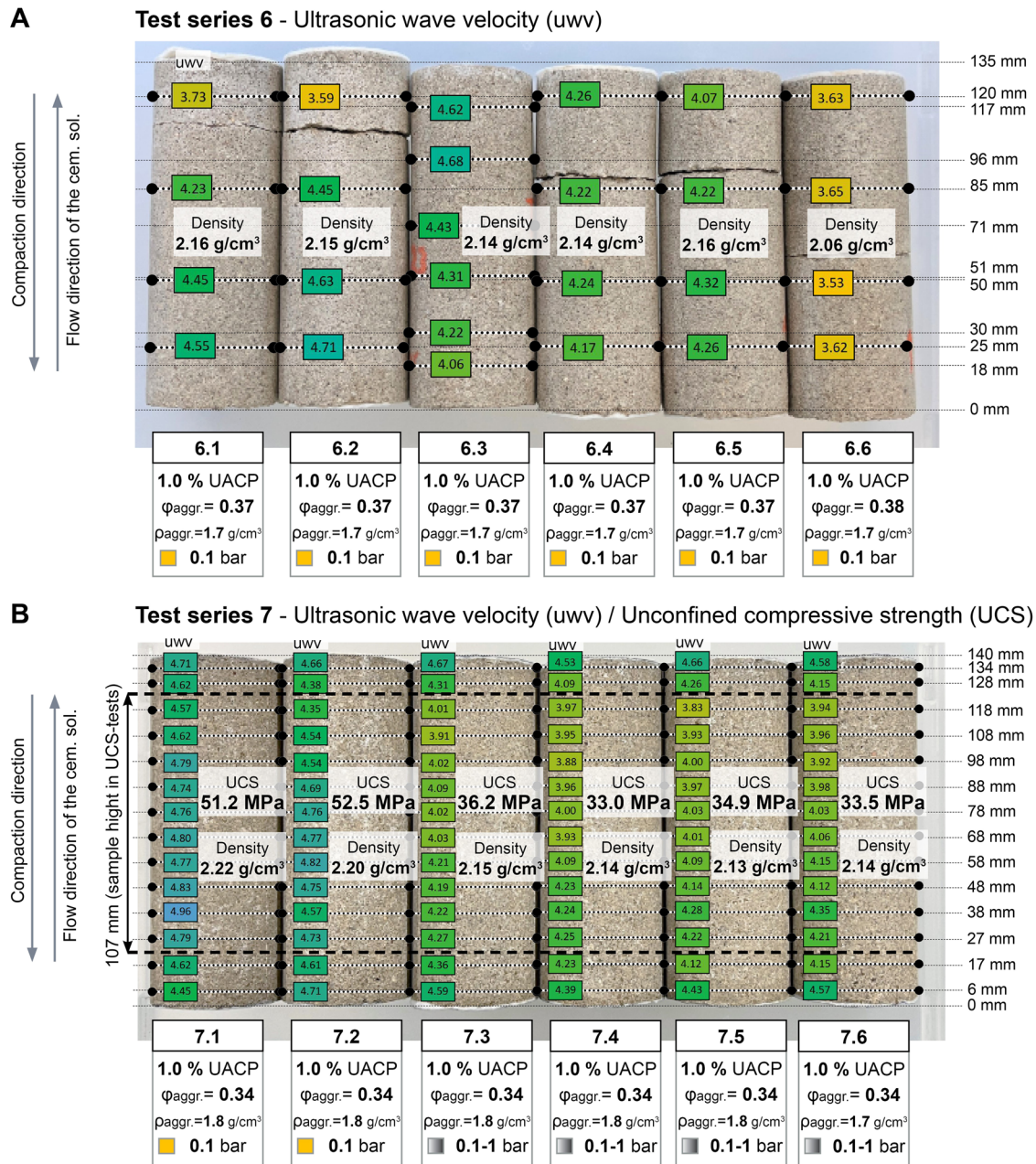


Fig. 5 The images of the produced specimens with the results of ultrasonic wave velocity measurements (*uwv, [km/s]) conducted at the marked points and the UCS-values obtained from the cut out samples ($D = 53.3$ mm, $H = 107$ mm). **A** Specimens produced in test series 6. **B** Specimens produced in test series 7.

of the produced specimens (Fig. 5A) also showed less homogeneous cementation in specimens 6.1 (3.73–4.55 km/s) and 6.2 (3.53–4.71 km/s) compared to the specimen 1.2 (4.50–4.64 km/s). The lowest ultrasonic wave velocities were observed in the specimen 6.6 with the highest value of $\phi_{\text{aggr.}} = 0.38$.

The cracks in the specimens of test series 6 visible in Fig. 5A likely occurred during removal of the specimens from the formworks using a hydraulic press, as significant pressure (sometimes up to 8 N/mm²) had to be applied during this operation. To facilitate easier specimen removal in the following test series 7 the PVC-pipes, which were cut open after biomineralization, were used instead of POM-cylinders as a formwork material. To ensure sufficient compaction quality in test series 7 the compaction pressure was increased to 10 N/mm². This resulted in a higher aggregate packing density with $\phi_{\text{aggr.}} = \text{ca. } 0.34$.

It was expected that with the higher aggregate packing density clogging might occur sooner during biomineralization, which would result in less homogeneous cementation. For this reason, a step-wise increase in the supply pressure of the cementation solution was applied during the biomineralization of the specimens 7.3 to 7.6. The pressure was increased from 0.1 bar to 0.4 bar after ca. 24 h, to 0.7 bar after ca. 44 h and to 1 bar after ca. 64 h. The specimens 7.1 and 7.2 were produced with a constant pressure of 0.1 bar.

The ultrasonic wave velocity measurements of the specimens produced in test series 7 revealed homogeneous cementation in all specimens (Fig. 5B). However, higher velocities, and thus higher densities, were observed in specimens 7.1 (4.45–4.90 km/s) and 7.2 (4.38–4.82 km/s), which were produced without step-wise pressure increase. These specimens also demonstrated higher overall

densities (2.20–2.22 g/cm³) and higher unconfined compressive strength values of 51.2 MPa and 52.5 MPa, compared to the specimens 7.3 to 7.6 (2.13–2.15 g/cm³, 33.0–36.2 MPa).

Generally, higher flow rates of the cementation solution were observed during biomineralization of the specimens with lower aggregate packing density (higher $\varphi_{\text{aggr.}}$ values) as shown in Fig. 6B. The maximal flow rate of ca. 33 ml/min occurred in the specimen 6.6 with $\varphi_{\text{aggr.}} = \text{ca. } 0.38$. The step-wise increase in supply pressure during biomineralization of the specimens 7.3, 7.4, 7.5 and 7.6 resulted in significant increases in flow rates at the corresponding time points. Considering the density, ultrasonic wave velocity, compressive strength and the fact that all specimens in test series 7 had similar aggregate packing density, it could be concluded that higher flow rates negatively affected the strength of the specimens 7.3 to 7.6 compared to the specimens 7.1 and 7.2 (Fig. 5B).

Calcium carbonate content in the samples taken from specimens 7.1, 7.2, 7.3, 7.4, 6.5 and 6.6 was similar for all specimens and ranged between ca. 15 and 22% (w/w) (Fig. 6C, E).

The estimated change in porosity during biomineralization was calculated based on the specimen weight increase (Fig. 6A), initial porosity and the density of CaCO₃ of 2.71 g/cm³ (Fig. 6D). Based on this estimation the flow rates were approaching a zero-value (Fig. 6B) when the porosity decreased to about 0.25.

It could be concluded that higher ultrasonic wave velocities and higher compressive strengths in test series 6 and 7 could be achieved in experiments with lower flow rates and higher aggregate packing density.

Environmental scanning electron microscopy (ESEM)

Environmental scanning electron microscopy (ESEM) images were obtained for different cross-sections of the specimens 1.2 [1.0% UACP, 0.1 bar, 0.75 M urea and CaCl₂] (top, middle, bottom) and 5.3 [1.5% UACP, 0.5 bar, 0.75 M urea and CaCl₂] (middle), which were cemented at the full height and displayed high ultrasonic wave velocities. The images (Fig. 7) reveal quartz sand grains (dark gray) coated with calcium carbonate (light gray), and void spaces (black). Interestingly, the layer of calcium carbonate, which could be observed at the locations, where sand grains were adjacent to voids, had approximately the same thickness in all images (ca. 20 μm thick). This indicated that the crystallization process initiated at the edges of the sand grains and presumably reached its growth limit at certain points of the biomineralization process. Similar calcium carbonate formations were also observed around some void spaces, presumably fluid or air bubbles.

A denser calcium carbonate coating was observed in the middle section of specimen 1.2 compared to the top and bottom sections. This variation could be attributed to the different availability of the UACP (ureolytic bacteria and calcium precursor) in different regions of the specimen. The top and bottom parts of the specimen were in direct contact with the hollow spaces of the formwork filled with the cementation solution, which may have resulted in reduced amounts of UACP in the top and bottom regions of the sample.

DISCUSSION

The unconfined compressive strength of biomineralized specimens generally increases with the increasing numbers of MICP-treatments due to the increasing CaCO₃ content¹⁶. This could be attributed to the formation of calcium carbonate bridges between the aggregates and the overall increase in density of the specimen. However, the density and consequently the UCS are also affected by the aggregate content, which stays constant throughout the biomineralization process. Although some studies attempted to compare the relationships between UCS and CaCO₃ content determined by different authors²³, such comparisons are

reasonable if identical aggregate matrices with the same grain sizes and the same packing density are used for biomineralization²⁴. In the present study we have shown that the density and, consequently, the UCS could also be increased by maximizing the aggregate content, along with the degree of cementation.

The calcium carbonate bonds might be a weaker constituent of bio-concrete than aggregates, because less stress is required to facilitate their breakage²⁰. This would also suggest that by maximizing the aggregate content the higher strength of bio-concrete could be achieved.

According to the own findings the unconfined compressive strength increases exponentially with the increasing density of the biomineralized specimens (Fig. 8A–C).

The stress-strain curve of the specimens from test series 7, presented in Fig. 6F, shows the plastic region at the stress level of ~4 MPa, where the deformation takes place under the constant load. After this a more elastic behavior is reestablished until the ultimate strength is reached. The presence of this region is unusual for concrete and could probably be attributed to the breakage of some calcium carbonate bridges and re-compaction of the aggregates²⁵. The plastic region at the low stress level could probably be eliminated through higher aggregate packing density.

The Young's modulus of the biomineralized specimens from test series 7 was assessed for the elastic regions of the stress-strain curves presented in Fig. 6F and is roughly equal to 11–12 GPa. Portland-cement-based concrete is generally stiffer and has an elastic modulus of about 20–50 GPa^{26,27}. With the corresponding density of ca. 2.2 g/cm³ the produced bio-concrete specimens fall into the domain of porous ceramics, along with concrete and bricks, as shown at the Ashby chart (Fig. 8D). To avoid excessive deformations in structures, the elastic modulus of bio-concrete could be increased by using coarse aggregates²⁸.

As mentioned in the "Results" section the incorporation of lime powder was also tested in order to further increase the aggregate packing density. Although a much higher aggregate packing density was achieved ($\varphi_{\text{aggr.}} = \text{ca. } 0.25$), there was no flow of the cementation solution observed when using the supply pressure of 0.1 bar. This result is consistent with the findings of the present study, as the flow rates were approaching a zero-value when the estimated porosity decreased to about 0.25 (Fig. 6F). Therefore, a higher supply pressure of the cementation solution is necessary for biomineralization of the mixes with the higher aggregate packing density.

However, by maximizing the aggregate content, it could also be necessary to minimize the surface to volume ratio of the aggregates. Too large surface area in case of the utilization of too fine aggregates in combination with the low amount of urease active material could result in the insufficient amount of calcium carbonate bonds produced between single grains. Increasing the amount of UACP up to 7.5% (w/w_{dm}) was tested in the present study and resulted in the poor cementation quality. The reason behind it could probably be related to the chemical kinetics and could not be fully explained in this study.

Increasing the supply pressure of the cementation solution generally resulted in deeper biomineralization when using higher UACP contents, because it allowed the chemicals in the cementation solution to reach parts of the specimen further away from the inlet without being consumed. Too high supply pressures and, consequently, too high flow rates had, however, a negative impact on the density and compressive strength of the specimens. Therefore, a production system with a precise control of the flow rates should be established for the production of bio-concrete.

Hydraulic press was used as a compaction tool in this study. The compaction technique for concrete should generally be selected in accordance to the consistency of the mix. The consistency class could be determined in a slump test²⁹. The presented bio-concrete mix exhibited, however, zero-slump behavior. According

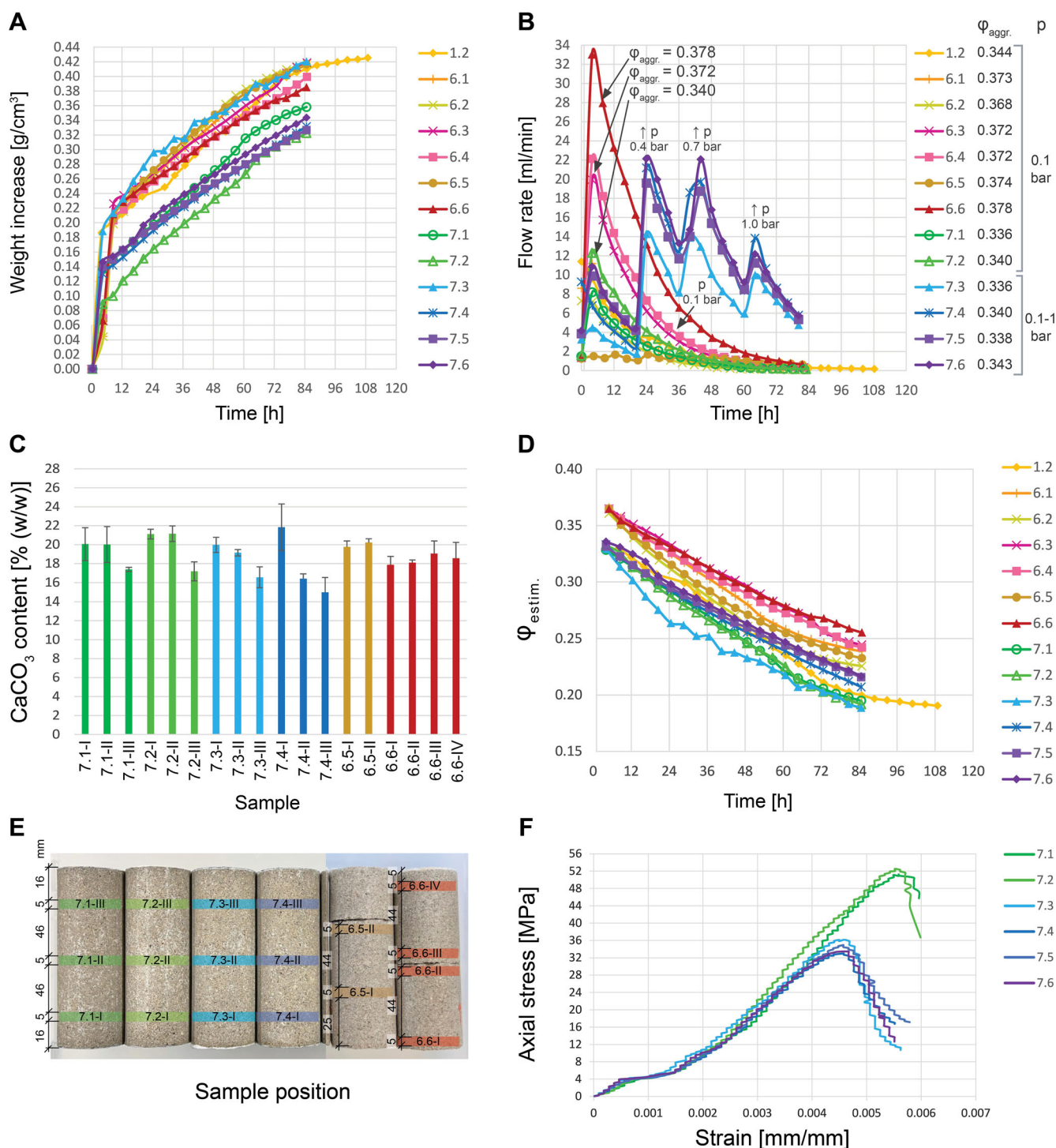


Fig. 6 Data obtained in test series 6 and 7 in comparison to the reference specimen 1.2. **A** Changes in specimen weights during biomineralization. **B** Changes in flow rates during biomineralization. **C** Measured CaCO₃ content of the finally obtained specimens. **D** Estimated change in porosity during biomineralization (based on the data from the graph A, initial porosity and the density of CaCO₃ of 2.71 g/cm³). **E** Positions of the samples within the specimens used for CaCO₃ measurements. **F** Stress-strain graphs of the samples from test series 7 during unconfined compressive stress tests.

to the recommendations of the association of the German cement industry (VDZ) stamping should be applied rather than vibration in this case³⁰. The best compaction results in the present study could be achieved by using hydraulic press. It is possible that combination of the pressing and vibration techniques could further improve the density of the mix, which would, however, require heavy vibration machinery.

The applied method demonstrated high reproducibility. This could be concluded from the similar rates of calcium carbonate production in test series 6 and 7 in comparison to the reference specimen 1.2 (Fig. 6A, C) and similar properties of the specimens produced with the same initial packing densities and the same cementation parameters (such as ultrasonic wave velocities, and,

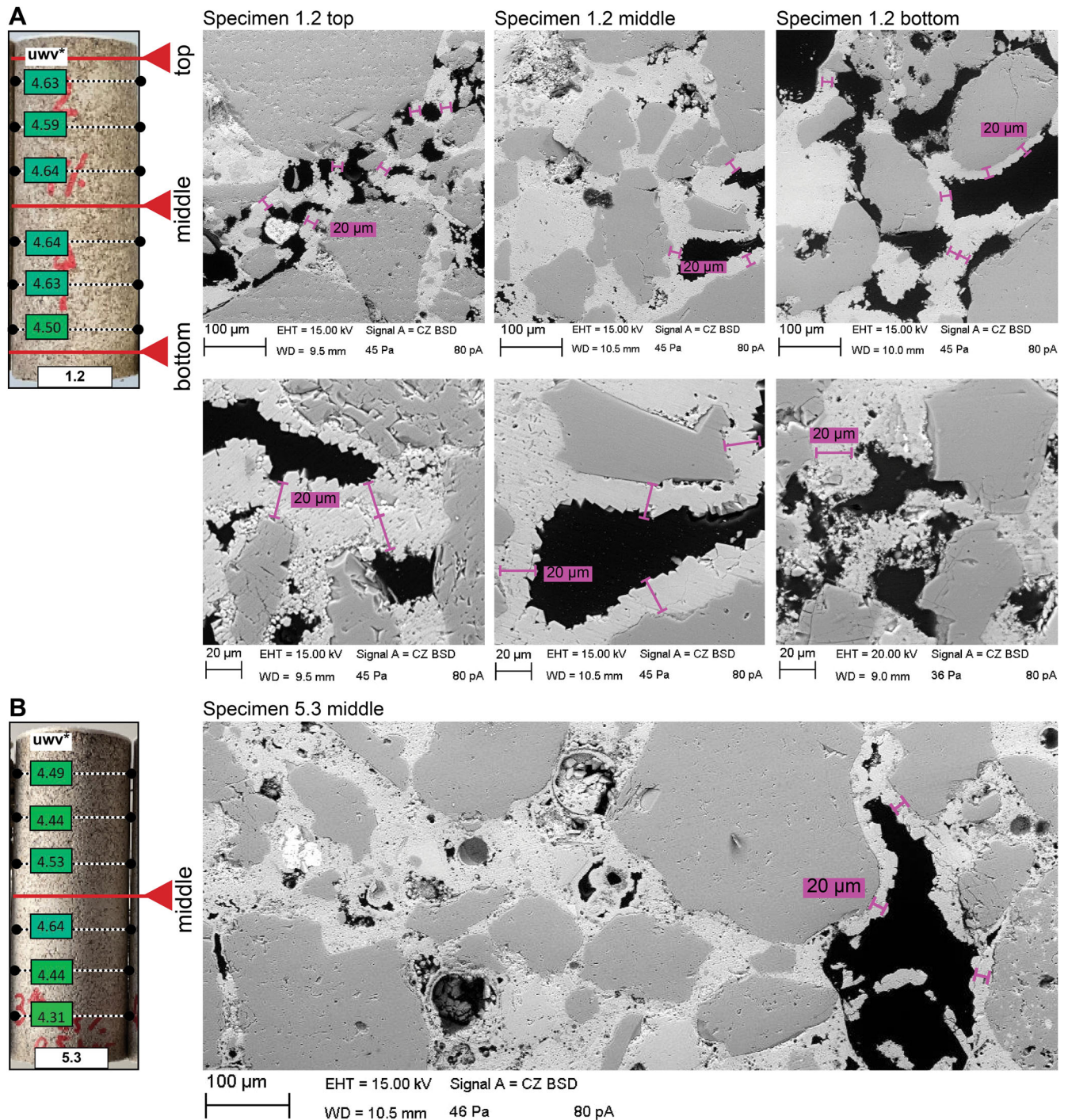


Fig. 7 ESEM images of polished cross-sections from different specimens. A Cross-sections from the top, middle and bottom parts of specimen 1.2. **B** Cross section from the middle part of specimen 5.3. The polished cross-sections were 5 mm thick and were cut out from the very top and bottom, as well as from the middle of the specimen. The corresponding images of the specimens with the ultrasonic wave velocity values at the marked points and the positions of the samples taken for the ESEM analysis (indicated by the red arrows) are provided on the left side of the figure.

consequently, similar local densities, unconfined compressive strengths and overall average densities (Fig. 5B)).

As a mineral material, bio-concrete needs to be reinforced when used in structural elements such as slabs. The corrosion of steel, a common reinforcement material, must be taken into consideration when using calcium chloride as a calcium source. While there are alternatives, such as calcium lactate or calcium acetate³¹,

which could be used for biomineralization, the higher availability of calcium chloride, particularly as a waste product from the Solvay process, and its low costs make it a favorable option. Corrosion resistant prestressed basalt fiber reinforcement could be used instead of steel in this case³².

The most favorable application of bio-concrete with the presented method could be the production of standardized

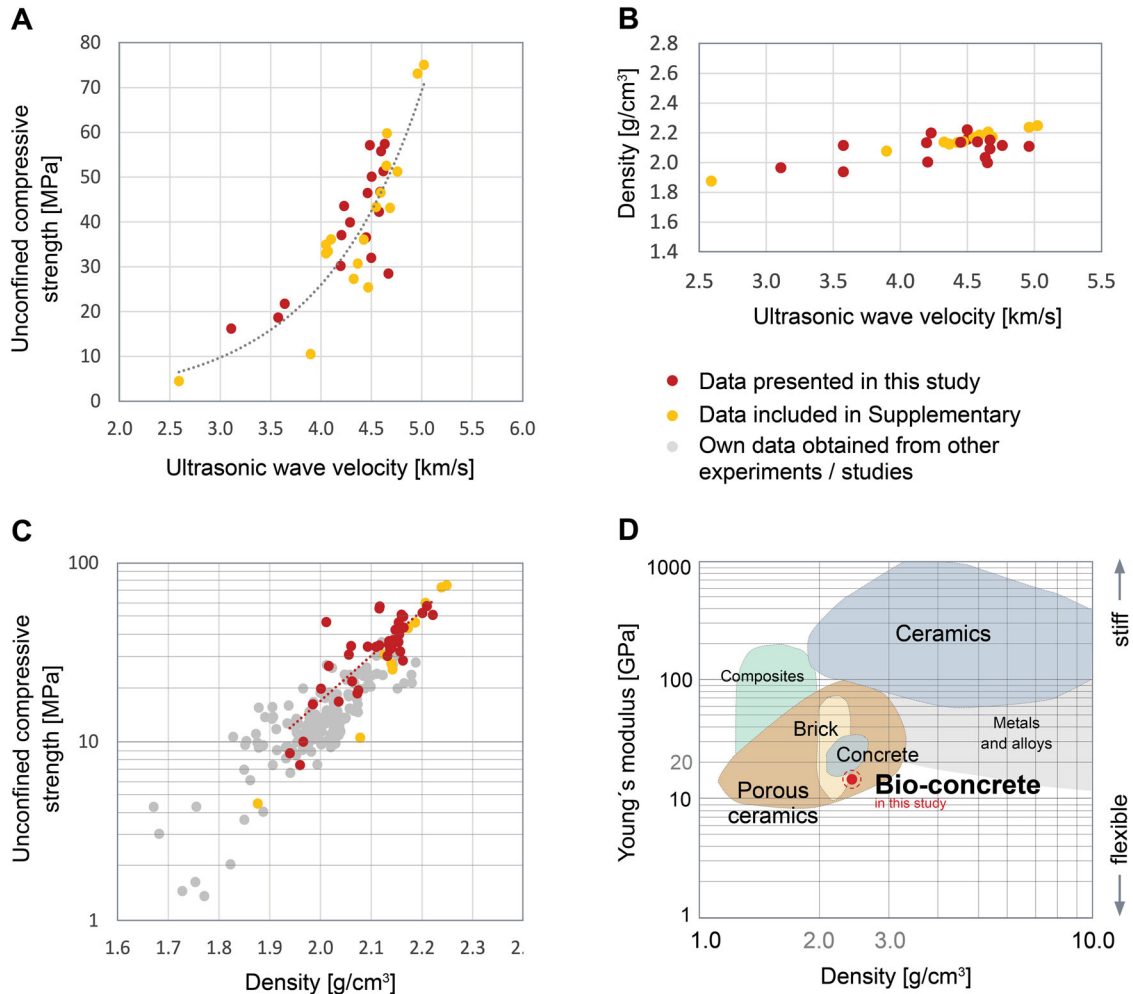


Fig. 8 Mechanical properties of bio-concrete. **A–C** Relationships between density, unconfined compressive strength and ultrasonic wave velocity of biomineralized specimens based on the data obtained from this study, data included in Supplementary and own data from other experiments. **D** Ashby chart showing the relationships between density and Young's modulus for different materials (redrawn from chart of the University of Cambridge⁴⁶).

prefabricated building components due to the necessity to feed the cementation solution into each individual formwork at specific time intervals.

Upscaling of the bio-concrete technology implies particular environmental challenges. Although the biomineralization process is CO₂-negative (carbon dioxide is stored in form of calcium carbonate) the sourcing of raw materials might be a cause of significant CO₂-emissions. For example, the production of industrial urea requires high temperature and pressure and is, therefore, energy intensive³³. Additionally, the carbon footprint of the production of raw materials could vary significantly depending on the energy source. One of the promising alternatives to the industrial urea is the utilization of urine for biomineralization³⁴.

Another challenge is recycling of the effluent solution. Releasing ammonium and chloride into the environment, particularly when calcium chloride is used as a calcium source, can definitely cause environmental harm. Apart from using the alternatives to calcium chloride³¹, all substances from the effluent solution could potentially be utilized for the production of new raw materials for bio-concrete³⁵ or be used in other industries (i.e., ammonium could be further processed to produce fertilizers). Therefore, choosing the raw materials and recycling options should be considered as parts of a combined material strategy in order to achieve carbon neutral bio-concrete production.

Apart from increasing the aggregate packing density the utilization of UACP instead of pure bacterial cultures could be another factor, which facilitated significant strength improvement achieved in this study. Nething et al. reported the UCS values up to 23 MPa when using a mix containing homogeneous fine sand and UACP¹⁹. This is higher than is being reported in the recent literature³⁶. By means of increasing the aggregate packing density in this study an even greater strength improvement (max. UCS 52.5 MPa in specimen 7.2 [$H/D = 2/1$] and 57.4 MPa in specimen 5.6 [$H/D = 1/1$]) has been achieved.

CONCLUSIONS

In the present study homogeneously cemented bio-concrete specimens were successfully produced using optimized mixes containing quartz sand with grain sizes from 0.63 to 2 mm and different amounts of UACP, which were biomineralized using pressure-based stop-flow injection method. The strongest and most homogeneously cemented specimens, with a height of 140 mm, exhibited the ultimate compressive strength values of 51.2–52.5 MPa ($\varphi_{\text{aggr.}} = \text{ca. } 0.34$). In general, compressive strength class of at least C20/25 (20 MPa for cylinder test specimens) of Portland-cement-based concrete is required for the production of prefabricated reinforced structural elements³⁷. The new findings

unveil the possibility to partially substitute traditional concrete with bio-concrete in this sector.

Such very high compressive strength values of biomineralized specimens in combination with a considerable cementation depth could be achieved by maximizing the aggregate content and adjusting the cementation parameters accordingly along with the utilization of UACP instead of pure bacterial cultures. This study encourages further development of the bio-concrete mix design by incorporating coarse aggregates and fines, which could open up further possibilities for the application of bio-concrete at a large scale.

METHODS

UACP preparation

Sporosarcina pasteurii. DSM33 was used throughout the experiments because it has been repeatedly shown this strain is highly alkalitolerant and synthesizes very high urease activities³⁸. The strain was purchased from the German Collection of Microorganisms and Cell Cultures GmbH (DSMZ, Germany). The organism was grown for 24 h at 30 °C under constant shaking (100 rpm) in a medium consisting of 10 g peptone from soymeal, 30 g peptone from casein, 5 g NaCl and 20 g urea per l (pH 7.3). The culture was grown to an optical density (at 600 nm) of about 5.

UACP was prepared from these cultures by the method of Cheng and Sahin¹⁸ by mixing a bacterial suspension with calcium chloride (0.4 M) and urea (0.4 M) under constant stirring. This resulted in the gradual enclosure of bacterial cells in calcium carbonate crystals formed through MICP (Supplementary Fig. 9). After settling, the moist bacterial calcium carbonate suspension was filtered and freeze-dried. Approximately 50 g of the UACP could be obtained from one liter of bacterial suspension using this procedure. UACP was vacuum packed and stored at −20 °C prior to the cementation experiments.

Media compounds were purchased from Roth (Germany). Chemicals and reagents were obtained from Roth (Germany), Diaclean (Germany) and Merck (Germany).

Urease activity of UACP

Urease activity in UACP samples was determined by measuring the release of ammonium from urea according to the method of Black et al.³⁹. Approximately 10 mg of UACP was transferred into a 2 ml reaction tube, the powder washed with 2 ml of 20 mM Tris/HCl buffer (pH 7.5) and centrifuged (2 min, 2000 × *g* at 4 °C). This process was repeated three times. After the last washing step, the UACP was resuspended in 1 ml of 20 mM Tris/HCl buffer (pH 7.5) using an ultrasonic bath for 10 min. The UACP suspension (12.5 μl) was mixed with 887.5 μl of 20 mM Tris/HCl buffer (pH 7.5) in a 2 ml reaction vessel, and the urease reaction was initiated by adding 100 μl of the urea solution (100 mM in 20 mM Tris/HCl buffer, pH = 7.5). The samples were mixed using a stirring bar and a magnetic stirrer at ~1000 rpm. Samples (120 μl) were taken after 0, 10, 20, and 30 min and centrifuged at 20,000 × *g* for 2 min each. The supernatants were used for the determination of ammonium ion concentration (see below). One unit (U) of urease activity was defined as the amount of urease which produced 1 μmol ammonium from urea per minute.

Mixing and compaction

The optimized sand mix (containing the following mass fractions: 19.5% [0.063–0.25 mm], 14.1% [0.1–0.4 mm], 10.9% [0.2–0.6 mm], 13.3% [0.3–0.8 mm], 17.2% [0.7–1.25], 25% [1.0–2.0]) was moistened with 10% (w/w) of the cementation solution (0.1 M calcium chloride, 0.1 M urea) in order to avoid segregation of different grain sizes. The resulting premix was prepared for 6 to 12 specimens. Subsequently, different amounts of UACP were added to

the portions of the premix (Supplementary Table 1 and Supplementary Fig. 10).

The mixes were stirred in a kneading machine (model: RMS7, manufacturer: GGM Gastro International GmbH) at 125 rpm for 2 min. Afterwards, the mixes were stirred by hand in order to lift the material deposited at the bottom of the mixing bowl and stirred in the machine for another 2 min.

In the next step, the mixes were compacted into cylindrical polyoxymethylene formworks in 10–20 mm layers using a hydraulic press. After compaction of each layer its surface was roughened with a sharp acrylic stick to ensure the adhesion of adjacent layers. A relatively high pressure of 5 N/mm² was chosen right from the beginning of the reported experiments. Further increasing the compaction pressure to 10 N/mm² in test series 7 has resulted in a higher compaction density.

In test series 1 to 6 the formworks had the shape of a truncated cone to allow the better removal of the specimens after the cementation (external $D = 60.0$ mm, internal $D_1 = 50.1$ mm, $D_2 = 51.7$ mm, $H = 150$ mm). In test series 7 the PVC pipes ($D = 53.3$ – 53.4 mm, $H = 150$ mm, wall thickness 4.7 mm) were used instead and were cut open after biomineralization. 3D-printed sieves (shown in Supplementary Fig. 10C) with fleece pads were installed into the formworks next to the inlets and outlets of the cementation solution. The resulting chambers provided the even distribution of the cementation solution throughout the contact surfaces of bio-concrete during biomineralization.

The volume ratios of the mix constituents and the mix pore volumes were determined by measuring the weight of the formworks before and after compaction. The grain density of UACP of 2.48 g/cm³ was estimated by a water displacement method. The density of the cementation solution (0.1 M calcium chloride, 0.1 M urea) of 1.0012 g/cm³ was calculated by weighing it in a 50-ml measuring cylinder.

Automated cementation system

The automated cementation system, shown in Fig. 2, was used to feed the cementation solution in the amount of one pore volume into the formworks filled with bio-concrete mixes every 4 h and to determine the weights of the formworks before each supply cycle. The system comprised a cementation solution supply unit, a scale unit, and a single-board computer (Raspberry Pi 4) for control and data collection. The schematic representation of the setup is provided in Supplementary Fig. 11 and its control logic in Supplementary Fig. 12. The system enabled the simultaneous cementation of six specimens in a single experiment.

The cementation solution supply unit consisted of the following components:

- three pressure tanks filled with different cementation solutions. The pressure in each tank was regulated separately through an attached pressure regulator. Each tank was connected to two formworks;
- six valves connected to the entry point of each formwork;
- six effluent beakers placed on six load cells;
- six peristaltic pumps for discharging the effluent beakers;
- control module with microcontroller (Arduino Mega), relays, drivers, etc.

At the beginning of the biomineralization experiment, a constant pressure was applied to the pressure tanks and maintained throughout the duration of the experiment. Every 4 h, corresponding to one cementation cycle, the cementation solution within the specimen was replaced by opening the entry valve. This caused the cementation solution to flow upward through the formwork. The cementation solution flowing out from the top of the formwork was collected in the effluent beaker, and its quantity was continuously recorded by the load cell (the data was processed using RS-485 standard with DMS amplifier from

Bosche Wägetechnik). Once the weight of the collected cementation solution matched the weight of the completely filled pore volume of the mixture in the formwork at the beginning of the cementation experiment (determined after the compaction process), the valve on the supply side of the formwork was closed. At the end of each cementation cycle, the solution was drained from the effluent beaker using a peristaltic pump.

The relatively low supply pressure of 0.1 bar was applied in test series 1. The supply pressures of the following test series were defined based on the results from the precedent experiments.

Formwork weight and flow rate during biomineralization

An automated scale unit was specifically designed to record the weight increase of the specimen during the biomineralization process. To mitigate the potential creep effects caused by continuous loading of the load cells with formworks over multiple days, a descending-lifting device controlled by a linear motor was incorporated into the scale unit. Prior to each cementation solution supply cycle, the formworks were lowered onto the load cells to be weighed and then lifted again afterwards.

The average flow rate for each cementation cycle was calculated using the data obtained from the corresponding load cell with the effluent beaker. Measurements were taken at intervals of ~5 s. Zero values recorded during periods when the valve was closed were disregarded in the calculation of the average flow rate.

Quantification of ammonium, calcium ions and urea in the effluent solution

Samples were taken from the effluent beakers at the end of the cementation cycles and used for the quantification of ammonium, calcium ions and urea.

The concentrations of ammonium, calcium ions, and urea were determined using photometric assays, which were adapted for the use in microtiter plates. The method for quantifying ammonium was described by Black et al.³⁹. The Spectroquant Calcium Cell Test from Merck, Germany, was used for the determination of calcium ion concentration. To determine the urea concentration, assays published by Jung et al.⁴⁰ and Phillips⁴¹ were employed. A detailed description of each of these assays is provided in Supplementary Methods.

Formwork removal and drying of the biomineralized specimens

Once all the cementation solution supply cycles were completed, the lids of the formworks were removed. The formworks, along with the specimens, were then dried at a temperature of 60 °C for a period of 48 h. Subsequently, the specimens were carefully pressed out of the formworks using a hydraulic press.

Ultrasonic wave velocity measurements

Ultrasound wave velocities were measured using an ultrasound wave generator (USG30, 46 kHz, sample rate 10 MHz, 16-fold sampling), a pair of transducers (UPG-D 3069, UPE-D 3066) and the LightHouse UMPC software, developed by Geotron-Elektronik, Germany. The used transducers are broadband 2 kHz to 100 kHz with a conical shape with punctiform contact points. Therefore, the beam angle can be considered almost 180°. Measurements were performed without coupling medium. The measurements were generally conducted along the height of the specimens, following the direction parallel to the compaction layers. The positions of the measurement points on the specimens are indicated in the Figures with the corresponding data in the results section. Additionally, for certain specimens, measurements were also taken in the direction perpendicular to the compaction layers. These measurements were taken after the specimens were cut for

the UCS tests and performed in accordance to testing standards DIN EN 12504-4:2021⁴² and DIN EN 14579:2004⁴³.

Cementation depth determination of the biomineralized specimens

Some specimens were not fully biomineralized. In this case the loose aggregates were removed and the cementation depth was determined by measuring the shortest distance between the farthest fully cemented cross-sections.

Unconfined compressive strength (UCS)

Most of the bio-concrete specimens displayed high inhomogeneity throughout their heights—a problem which generally does not occur when working with ordinary Portland-cement-based concrete. Therefore, the diameter to height ratio 1:1 (in compliance with the testing standard for natural stone DIN EN 1926⁴⁴) was chosen to compare the UCS in different parts of the specimens in test series 1 to 5. If the cementation depth was sufficient one or two cylinders with the height of 50–60 mm (diameter to height ratio of approx. 1:1) were cut out of each specimen.

The specimens in test series 7 were homogeneously cemented, which enabled to test the samples with the diameter to height ratio 2:1 (in compliance with³⁷).

The UCS of the cylinders was measured with a path-controlled application of the axial load at a constant rate of 0.5 mm/min. The tests were conducted on the testing machine SP-SRG 5000 and the testing frame ZDEM 20/600 (Walter + Bai AG, Switzerland) using the software Proteus MT (FORM + TEST Seidner & Co. GmbH, Germany).

Calcium carbonate content of the biomineralized specimens

The carbonate content of the biomineralized specimens was determined by employing a pressure-calimeter method as outlined by Sherrod et al.⁴⁵. First, the samples were pounded in a stainless steel mortar using a stainless pestle. The crushed samples (1.2–1.5 g) were transferred to screwable glass bottles (100 ml). Then, vials containing 6 ml of 6 M HCl were added to the bottles. Bottles were closed airtight with caps containing a quick connection, which allowed to connect the reaction vessels to a digital pressure sensor. The closed bottles were shaken to spill the acid within the reaction vessels, which allowed the acid to react with the pounded samples thus leading to CO₂ release from the samples. The resulting increase in pressure was recorded as the voltage response of the pressure sensor using a digital voltmeter. The carbonate content of each sample was measured in triplicates. Calibration curves were generated using defined amounts of CaCO₃ (0.02–0.4 g).

Environmental scanning electron microscopy (ESEM)

Cross section samples were prepared for the selected specimens. The samples were ~5 mm thick and were cut out from the very top, the very bottom and the middle of the biomineralized specimens with a height of 135 mm. Subsequently, the samples were soaked with an epoxy resin (Araldite 2020), polished and analyzed by scanning electron microscopy (Zeiss EVO LS15; EHT (extra high tension) of 20 kV and CZ BSD (back scattered detection)).

DATA AVAILABILITY

The datasets generated during and/or analyzed during the current study are available from the corresponding author on reasonable request.

Received: 11 July 2023; Accepted: 13 November 2023;
Published online: 13 December 2023

REFERENCES

- International Energy Agency (IEA). *Cement*. <https://www.iea.org/energy-system/industry/cement> (2023).
- Global Cement and Concrete Association (GCCA). *Global Cement and Concrete Industry Announces Roadmap to Achieve Groundbreaking "Net Zero" CaCO₂ Emissions by 2025*. <https://gccassociation.org/news/global-cement-and-concrete-industry-announces-roadmap-to-achieve-groundbreaking-net-zero-co2-emissions-by-2050/> (2023).
- Preston, F. & Lehne, J. *Making Concrete Change: Innovation in Low-carbon Cement and Concrete* (The Royal Institute of International Affairs, 2018).
- Castro-Alonso, M. J. et al. Microbially induced calcium carbonate precipitation (MICP) and its potential in bioconcrete: microbiological and molecular concepts. *Front. Mater.* **6**, 126 (2019).
- Achal, V. & Pan, X. Characterization of urease and carbonic anhydrase producing bacteria and their role in calcite precipitation. *Curr. Microbiol.* **62**, 894–902 (2011).
- Blakeley, R. L., Hinds, J. A., Kunze, H. E., Webb, E. C. & Zerner, B. Jack bean urease (EC 3.5.1.5). demonstration of a carbamoyl-transfer reaction and inhibition by hydroxamic acids. *Biochemistry* **8**, 1991–2000 (1969).
- Zehner, J., Røyne, A., Wentzel, A. & Sikorski, P. Microbial-induced calcium carbonate precipitation: an experimental toolbox for in situ and real time investigation of micro-scale pH evolution. *RSC Adv.* **10**, 20485–20493 (2020).
- Ghosh, T., Bhaduri, S., Montemagno, C. & Kumar, A. *Sporosarcina pasteurii* can form nanoscale calcium carbonate crystals on cell surface. *PLoS ONE* **14**, e0210339 (2019).
- Hossain, M. R. et al. Self-healing concrete for sustainable buildings. a review. *Environ. Chem. Lett.* **20**, 1265–1273 (2022).
- Harran, R., Terzis, D. & Laloui, L. Mechanics, modeling, and upscaling of bio-cemented soils: a review of breakthroughs and challenges. *Int. J. Geomech.* **23**, 03123004 (2023).
- Cheng, L., Kobayashi, T. & Shahin, M. A. Microbially induced calcite precipitation for production of "bio-bricks" treated at partial saturation condition. *Constr. Build. Mater.* **231**, 117095 (2020).
- Bu, C., Wen, K., Liu, S., Ogbonnaya, U. & Li, L. Development of bio-cemented constructional materials through microbial induced calcite precipitation. *Mater. Struct.* **51**, 30 (2018).
- Zhang, K. et al. Microbial induced carbonate precipitation (MICP) technology: a review on the fundamentals and engineering applications. *Environ. Earth Sci.* **82**, 229 (2023).
- Konstantinou, C., Biscontin, G., Jiang, N.-J. & Soga, K. Application of microbially induced carbonate precipitation to form bio-cemented artificial sandstone. *J. Rock Mech. Geotech. Eng.* **13**, 579–592 (2021).
- Harkes, M. P., van Paassen, L. A., Booster, J. L., Whiffin, V. S. & van Loosdrecht, M. C. Fixation and distribution of bacterial activity in sand to induce carbonate precipitation for ground reinforcement. *Ecol. Eng.* **36**, 112–117 (2010).
- Konstantinou, C., Wang, Y., Biscontin, G. & Soga, K. The role of bacterial urease activity on the uniformity of carbonate precipitation profiles of bio-treated coarse sand specimens. *Sci. Rep.* **11**, 6161 (2021).
- Cheng, L. & Cord-Ruwisch, R. Upscaling effects of soil improvement by microbially induced calcite precipitation by surface percolation. *Geomicrobiol. J.* **31**, 396–406 (2014).
- Cheng, L. & Shahin, M. A. Urease active bioslurry: a novel soil improvement approach based on microbially induced carbonate precipitation. *Can. Geotech. J.* **01**, 1376–1385 (2016).
- Nething, C. et al. A method for 3d printing bio-cemented spatial structures using sand and urease active calcium carbonate powder. *Mater. Des.* **195**, 109032 (2020).
- Xiao, Y. et al. Compression behavior of MICP-treated sand with various gradations. *Acta Geotech.* **16**, 1391–1400 (2021).
- Bernardi, D., DeJong, J., Montoya, B. & Martinez, B. Bio-bricks: biologically cemented sandstone bricks. *Constr. Build. Mater.* **55**, 462–469 (2014).
- Kahl, W.-A., Hinkes, R., Feeser, V. & Holzheid, A. Microfabric and anisotropy of elastic waves in sandstone—an observation using high-resolution x-ray microtomography. *J. Struct. Geol.* **49**, 35–49 (2013).
- Lai, H., Wu, S., Cui, M. & Chu, J. Recent development in biogeotechnology and its engineering applications. *Front. Struct. Civil Eng.* **15**, 1073–1096 (2021).
- Xiao, Y., He, X., Zaman, M., Ma, G. & Zhao, C. Review of strength improvements of bio-cemented soils. *Int. J. Geomech.* **22**, 03122001 (2022).
- Harran, R., Terzis, D. & Laloui, L. Characterizing the deformation evolution with stress and time of bio-cemented sands. *J. Geotech. Geoenviron. Eng.* **148**, 04022074 (2022).
- Krizova, K. & Hela, R. Evaluation of static modulus of elasticity depending on concrete compressive strength. *Int. J. Civil Environ. Eng.* **9**, 654–657 (2015).
- Beushausen, H. & Dittmer, T. The influence of aggregate type on the strength and elastic modulus of high strength concrete. *Constr. Build. Mater.* **74**, 132–139 (2015).
- Zhou, F. P., Lydon, F. D. & Barr, B. I. G. Effect of coarse aggregate on elastic modulus and compressive strength of high performance concrete. *Cem. Concr. Res.* **25**, 177–186 (1995).
- German Institute for Standardisation (DIN). *DIN EN 206:2021-06, Concrete—Specification, Performance, Production and Conformity; German version* (Beuth Verlag GmbH, Berlin, 2021).
- German Cement Works Association (VDZ). *Zement-Merkblatt B7: Bereiten und Verarbeiten von Beton*. <https://www.vdz-online.de/wissensportal/publikationen/zement-merkblatt-b7-bereiten-und-verarbeiten-von-beton> (2023).
- Røyne, A. et al. Towards a low CO₂ emission building material employing bacterial metabolism (1/2): the bacterial system and prototype production. *PLoS ONE* **14**, e0212990 (2019).
- Blandini, L. *Lightweight and Sustainable Concrete Structures: The ILEK Research Strategy in Proceedings of the 6th fib International Congress* (Fédération Internationale du Béton, 2022).
- Fouladi, A. S., Arulrajah, A., Chu, J. & Horpibulsuk, S. Application of microbially induced calcite precipitation (MICP) technology in construction materials: a comprehensive review of waste stream contributions. *Constr. Build. Mater.* **388**, 131546 (2023).
- Lambert, S. E. & Randall, D. G. Manufacturing bio-bricks using microbial induced calcium carbonate precipitation and human urine. *Water Res.* **160**, 158–166 (2019).
- Dosier, G. K., Dosier, J. M. & Smith, K. J. US Patent 20190106716A1 (2019).
- Fu, T., Saracho, A. C. & Haigh, S. K. Microbially induced carbonate precipitation (MICP) for soil strengthening: a comprehensive review. *Biogeotechnics* **1**, 100002 (2023).
- German Institute for Standardization (DIN). *DIN EN 13369:2018-09, Common Rules for Precast Concrete Products; German Version* (Beuth Verlag GmbH, 2018).
- Wu, Y., Li, H. & Li, Y. Biomineralization induced by cells of *sporosarcina pasteurii*: mechanisms, applications and challenges. *Microorganisms* **9**, 2396 (2021).
- Black, G. W. et al. A high-throughput screening method for determining the substrate scope of nitrilases. *Chem. Commun.* **51**, 2660–2662 (2015).
- Jung, D., Biggs, H., Erikson, J. & Ledyard, P. U. New colorimetric reaction for end-point, continuous-flow, and kinetic measurement of urea. *Clin. Chem.* **21**, 1136–1140 (1975).
- Phillips, A. J. *Biofilm-Induced Calcium Carbonate Precipitation: Application in the Subsurface*. PhD thesis (Montana State University, Bozeman, College of Engineering, 2013).
- German Institute for Standardization (DIN). *DIN EN 12504-4:2021-10, Testing Concrete in Structures—Part 4: Determination of Ultrasonic Pulse Velocity; German Version EN 12504-4:2021* (Beuth Verlag GmbH, 2021).
- German Institute for Standardization (DIN). *DIN EN 14579:2005-01, Natural Stone Test Methods—Determination of Sound Speed Propagation; German Version EN 14579:2004* (Beuth Verlag GmbH, 2005).
- German Institute for Standardization (DIN). *DIN EN 1926:2007-03, Natural Stone Test Methods—Determination of Uniaxial Compressive Strength; German Version* (Beuth Verlag GmbH, 2017).
- Sherrod, L. A., Dunn, G., Peterson, G. A. & Kolberg, R. L. Inorganic carbon analysis by modified pressure-calimeter method. *Soil Sci. Soc. Am. J.* **66**, 299–305 (2002).
- University of Cambridge, Department of Engineering. *Material Selection and Processing*. <http://www-materials.eng.cam.ac.uk/mpsite/default.html> (2023).

ACKNOWLEDGEMENTS

This study was funded by the German Federal Institute for Research on Building, Urban Affairs and Spatial Development (grant number 10.08.18.7-20.41) and the Ministry of the Environment, Climate Protection and the Energy Sector Baden-Württemberg, Germany (grant number L75 22102). The funders played no role in study design, data collection, analysis and interpretation of data, or the writing of this manuscript.

AUTHOR CONTRIBUTIONS

M.S. and C.N. prepared and conducted the biomineralization experiments. J.G. and D.F. quantified ammonium, calcium and urea in effluent solutions. E.E. and D.F. prepared UACP and measured its urease activity. M.R. conducted ultrasonic wave velocity measurements and environmental scanning electron microscopy. J.G., E.E. and D.F. conducted calcium carbonate measurements on the dried specimens. M.S. wrote the main manuscript text and prepared figures. A.S. edited the main manuscript text. All authors reviewed the manuscript. A.S., J.F. and L.B. provided laboratory equipment and resources.

FUNDING

Open Access funding enabled and organized by Projekt DEAL.

COMPETING INTERESTS

The authors declare no competing interests.

ADDITIONAL INFORMATION

Supplementary information The online version contains supplementary material available at <https://doi.org/10.1038/s44296-023-00004-6>.

Correspondence and requests for materials should be addressed to Christoph Nething.

Reprints and permission information is available at <http://www.nature.com/reprints>

Publisher's note Springer Nature remains neutral with regard to jurisdictional claims in published maps and institutional affiliations.



Open Access This article is licensed under a Creative Commons Attribution 4.0 International License, which permits use, sharing, adaptation, distribution and reproduction in any medium or format, as long as you give appropriate credit to the original author(s) and the source, provide a link to the Creative Commons license, and indicate if changes were made. The images or other third party material in this article are included in the article's Creative Commons license, unless indicated otherwise in a credit line to the material. If material is not included in the article's Creative Commons license and your intended use is not permitted by statutory regulation or exceeds the permitted use, you will need to obtain permission directly from the copyright holder. To view a copy of this license, visit <http://creativecommons.org/licenses/by/4.0/>.

© The Author(s) 2023